Bulletin of the Seismological Society of America, Vol. 79, No. 2, pp. 304–329, April 1989

BEHAVIOR OF THE SUPERSTITION HILLS FAULT DURING THE PAST 330 YEARS

BY K. W. HUDNUT AND K. E. SIEH

ABSTRACT

We have investigated the recent prehistoric behavior of the Superstition Hills fault by examining its effect on the beach deposits of ancient Lake Cahuilla. Excavation of these sediments in three dimensions where they are cut by the fault has enabled determination of total offset since the latest highstand of the lake, about 330 years ago. As of 3 March 1988, total dextral offset was 1106 ± 50 mm. About 609 mm of this amount can be attributed to one or more slip events before 1987. The remaining slip occurred during the moderate earthquake of 24 November 1987 and as subsequent aftercreep. Additional aftercreep here might produce a total of 1210 ± 100 mm for that event. Thus, if afterslip continues according to our prediction, slip associated with the penultimate seismic slip event on the Superstition Hills fault was only about half of the co-seismic slip and predicted afterslip associated with the 1987 earthquake. This difference, established at a single site on the fault, may reflect a larger size for the 1987 event than for its predecessor. We calculate that the slip rate of the Superstition Hills fault zone, averaged over the past 330 years, is between about 2 and at least 6 mm/yr at this site. During this time, the average interval between large surface slip events on the Superstition Hills fault has been between about 150 and 300 years. The pre-1987 slip event documented in our excavations could have occurred at any time between A.D. 1660 and about A.D. 1915. These results are significant for understanding earthquake recurrence and patterns of earthquakes in the Imperial and Coachella Valleys.

INTRODUCTION

The Superstition Hills fault is a strand of the San Jacinto fault zone. Figure 1 shows its position adjacent to the Superstition Mountain fault and between parts of the Coyote Creek fault that ruptured during the earthquake of 1968, and the Imperial fault that ruptured during earthquakes in 1940 and 1979. Northeast of the Superstition Hills fault are at least three major cross-faults that trend northeastward, toward the Brawley seismic zone. One of these ruptured during the strongest aftershock of the 1979 event (Johnson and Hutton, 1982), another ruptured during the Westmorland earthquake of 1981 (Nicholson *et al.*, 1986), and others broke during the largest foreshock (M_S = 6.2) of the 24 November 1987 earthquake sequence, 11.4 hr before the main shock (M_S = 6.6) rupture of the Superstition Hills fault.

Before the 1987 earthquake, the potential of the Superstition Hills fault to produce moderate earthquakes had not been established. This fault was suggested as a possible source for the 19 April 1906 event or the two moderate earthquakes of 23 June 1915 (Toppozada and Parke, 1982; Anderson and Bodin, 1987). Other sources for these quakes were also considered possible, however, because epicentral location was very poorly constrained.

Sieh (1982) hypothesized that the Superstition Hills fault would be among the next to produce a moderate earthquake in the region. This suggestion was based on the observation that the section of the Imperial fault that had experienced triggered slip associated with the 1968 Borrego Mountain earthquake was almost the same

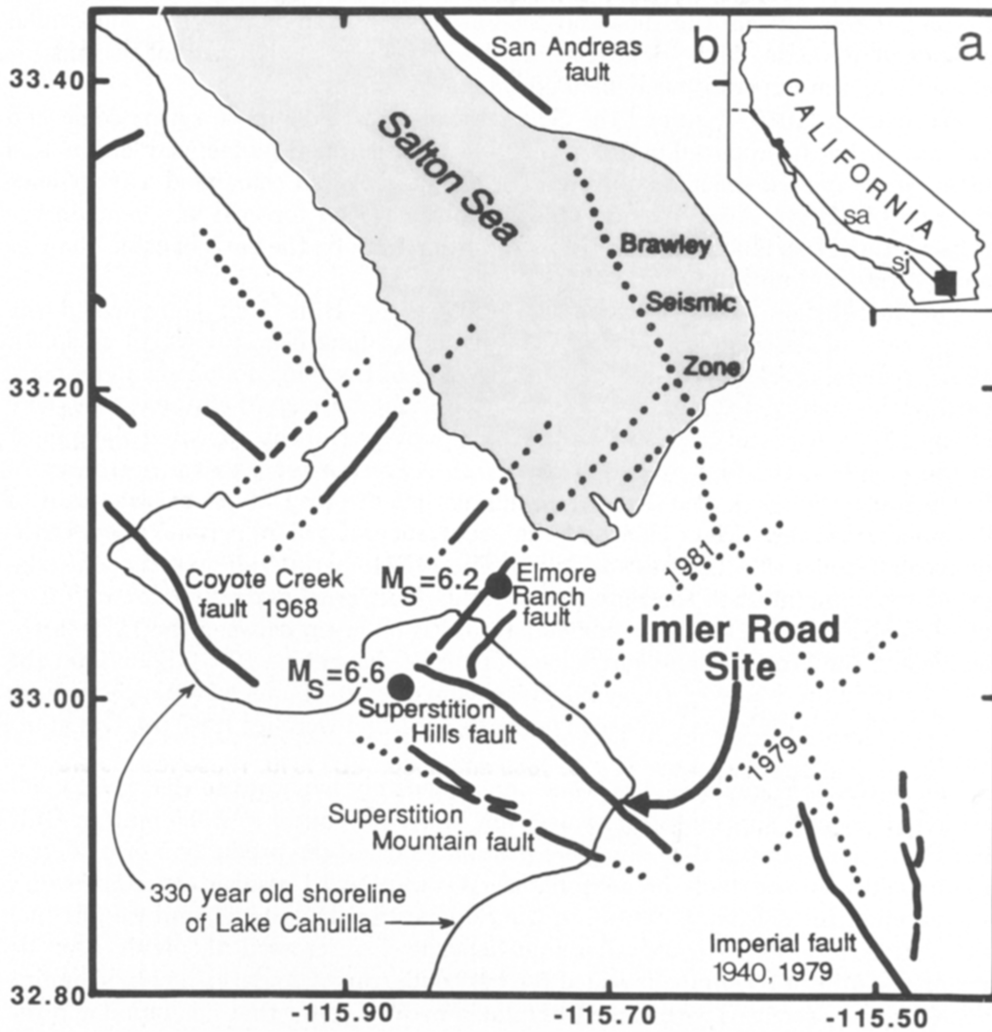

FIG. 1. (a) Generalized map of the San Andreas fault (sa) and San Jacinto fault zone (sj) in California. (b) Tectonic setting of the Superstition Hills fault. The ancient (330 year BP) shoreline of Lake Cahuilla follows the southwest margin of the Salton trough. It crosses the southern part of the Superstition Hills fault at our study site near Imler road. Dotted lines are faults inferred from seismicity and/or basement structure (Fuis *et al.*, 1984). Dates of major earthquakes on the faults are shown, and cross-faults that ruptured in 1979 and 1981 are also indicated.

segment that ruptured co-seismically in 1979. Observations of triggered slip on the Superstition Hills fault and the southern 40 km of the San Andreas fault in 1968 and 1979 led him then to speculate that these two faults would be the next to break.

Sykes and Nishenko (1984), however, hypothesized that moderate earthquakes in 1942 and 1954 ruptured from the south end of the 1968 Coyote Creek fault break southward, to the south terminus of the San Jacinto fault zone, yielding low probability estimates for rupture of the Superstition Hills fault and the subparallel Superstition Mountain fault.

Relocation of the 1942 earthquake to the southwest of the San Jacinto fault zone, and of the 1954 event onto the Clark fault strand by Sanders *et al.* (1986) had two effects on these predictions. First, it suggested the possibility that the southernmost San Jacinto fault zone had experienced no ruptures during the past ~70 years.

Second, it showed that the 1954 and 1968 breaks occurred on adjacent, subparallel strands of the zone. Thus, Sanders *et al.* (1986) removed two potential reasons for considering the Superstition Hills fault a low-risk segment.

Wesnousky (1986) assumed the Superstition Hills fault to be seismogenic and estimated that it produced events of $M_L = 6.4$, based upon its mapped length, and using an estimated seismic slip rate of 1 mm/yr, he then calculated a recurrence interval of 422 yr. Also, Wesson and Nicholson (1988) forecast an event on the Superstition Hills fault or Superstition Mountain fault on the basis of creep changes along strike and unusual seismicity.

The recognition of creep along the Superstition Hills fault complicated the assessment of its seismic potential. The fault had long been known to creep. In 1951, surficial cracks were observed on a section of the fault, following a moderate earthquake nearby (Dibblee, 1954). Shortly after the Borrego Mountain earthquake of April 1968, surficial cracks with up to 18 mm of dextral slip appeared along most of the length of the fault (Allen *et al.*, 1972). A creepmeter 3.15 km northwest of Imler Road (Fig. 2a) recorded the accumulation of creep at an average rate of 0.5 mm/yr between May 1968 and the occurrence of the Imperial Valley earthquake in October 1979 (Louie *et al.*, 1985). The 1979 Imperial Valley earthquake triggered slip along most of the Superstition Hills fault, with maximum dextral offset of 22 mm (Fuis, 1982). The creepmeter recorded no creep between the 1979 earthquake and the Westmorland earthquake of 1981 (Louie *et al.*, 1985). Soon after the 1981 earthquake, however, triggered dextral slip of up to 15 mm was mapped (Sharp *et al.*, 1986). No creep was recorded between 1981 and October 1987 (McGill *et al.*, 1989).

Before the earthquake of 1987, one could plausibly hypothesize that the Superstition Hills fault slipped solely by aseismic creep at about 0.75 ± 0.5 mm/yr. Only if a higher long-term rate of slip were postulated could the production of moderate earthquakes by the fault be reasonable. We wanted to resolve the controversy surrounding the seismic potential of the Superstition Hills fault, and we felt that excavation of ~300-year-old shoreline deposits that crossed the fault near its mapped southern terminus provided the best opportunity to do so. These shoreline deposits are associated with Lake Cahuilla, a body of water that has inundated the Imperial, Mexicali, Coachella, and Lower Borrego Valleys to an elevation of about 13 m above mean sea level (msl) at least five times in the past millenium (Waters, 1983; Sieh, 1987). The most recent filling occurred about A.D. 1663 ±22 (Sieh and Williams, manuscript in preparation).

Our initial intention was to determine the magnitude of dextral offset of these deposits. Offsets greater than about 300 mm would have led us to support co-seismic rupture in the past 330 years, or pre-1967 aseismic creep rates higher than the average rate observed since then of about 0.9 mm/yr. Lesser offset would have implied pre-1967 aseismic creep at rates equal to or less than the measured rates. The November 1987 earthquake answered our initial question: the fault does produce moderate earthquakes. Furthermore, the occurrence of the earthquake provided us with a new set of problems to approach through paleoseismic studies.

The principal new questions are these: Have other co-seismic ruptures of this fault occurred during the past 300 years? And, if they have, were offsets similar to those associated with the earthquake of 1987? This seemed likely, because the Superstition Hills fault with its apparently well-defined termini (Allen *et al.*, 1972; Fuis, 1982; Dibblee, 1984) seemed a likely candidate for the generation of characteristic earthquakes (Schwartz and Coppersmith, 1984).

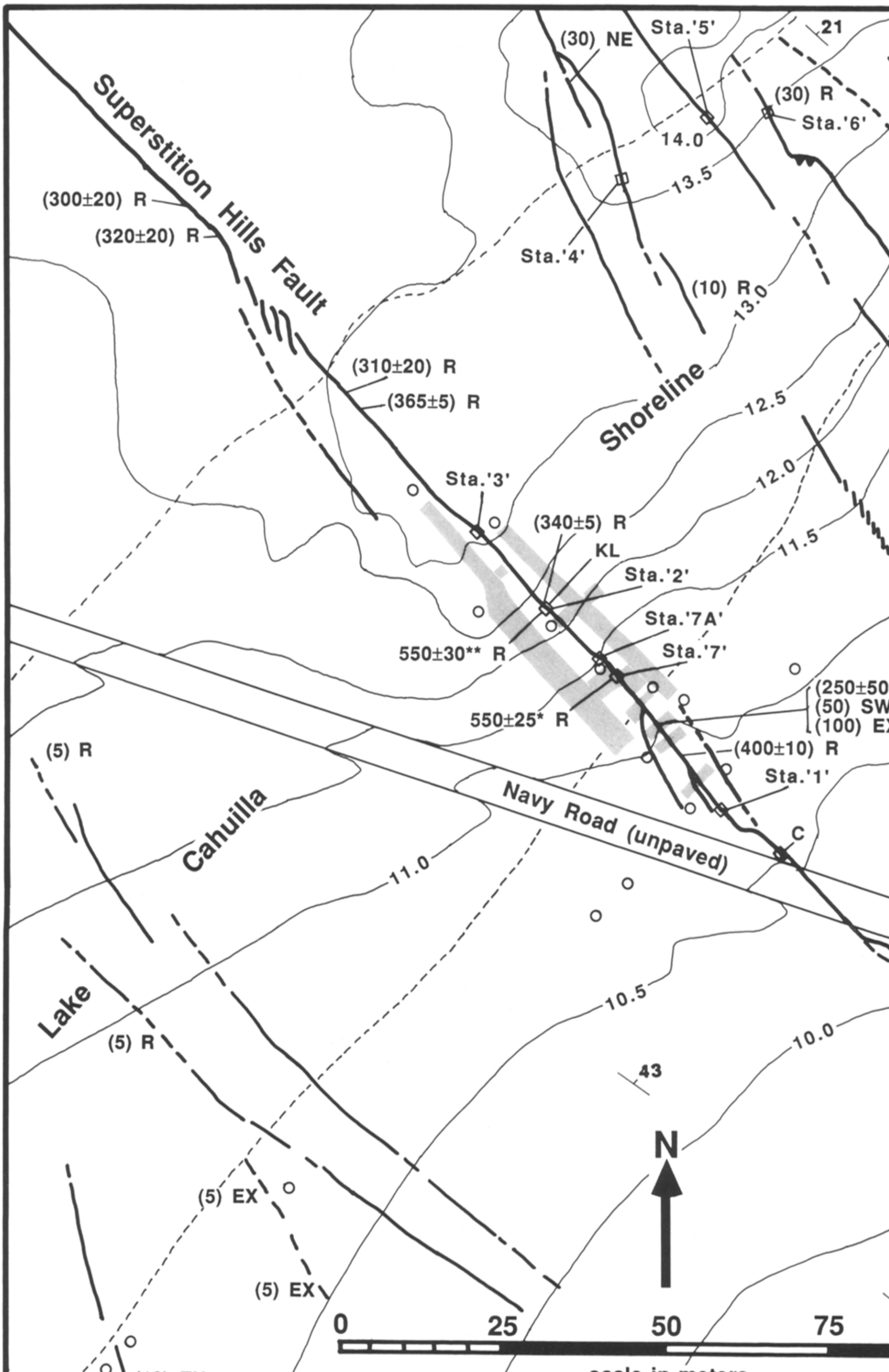

FIG. 2. a) Inset map showing the 1987 rupture trace on the Superstition Hills fault (SHF), as mapped by Kahle *et al.* (1988), on either side of our study site. The fault ruptured through the geomorphically expressed curvilinear berm of Lake Cahuilla shoreline deposits about 250 m northwest of Imler Road. The Caltech creepmeter is indicated by 'CIT', and the CIT alinement array near the excavations is shown. The location of Bilham's creepmeter, where afterslip was measured, is identified by 'RB': Williams and Magistrales's afterslip measurement sites, '2T' and '2U', are also labelled. b) Site map of our excavations near Imler Road on the Superstition Hills fault. Mapped features include surface ruptures associated with the earthquake of November 1987, topography of the site (plane-table mapped using the Zeiss Elta-4 surveying instrument on March 10, 1988), afterslip monitoring markers (KL, C, and Sta. 1 through 7, 7A), survey benchmarks, and the locations of our excavations.

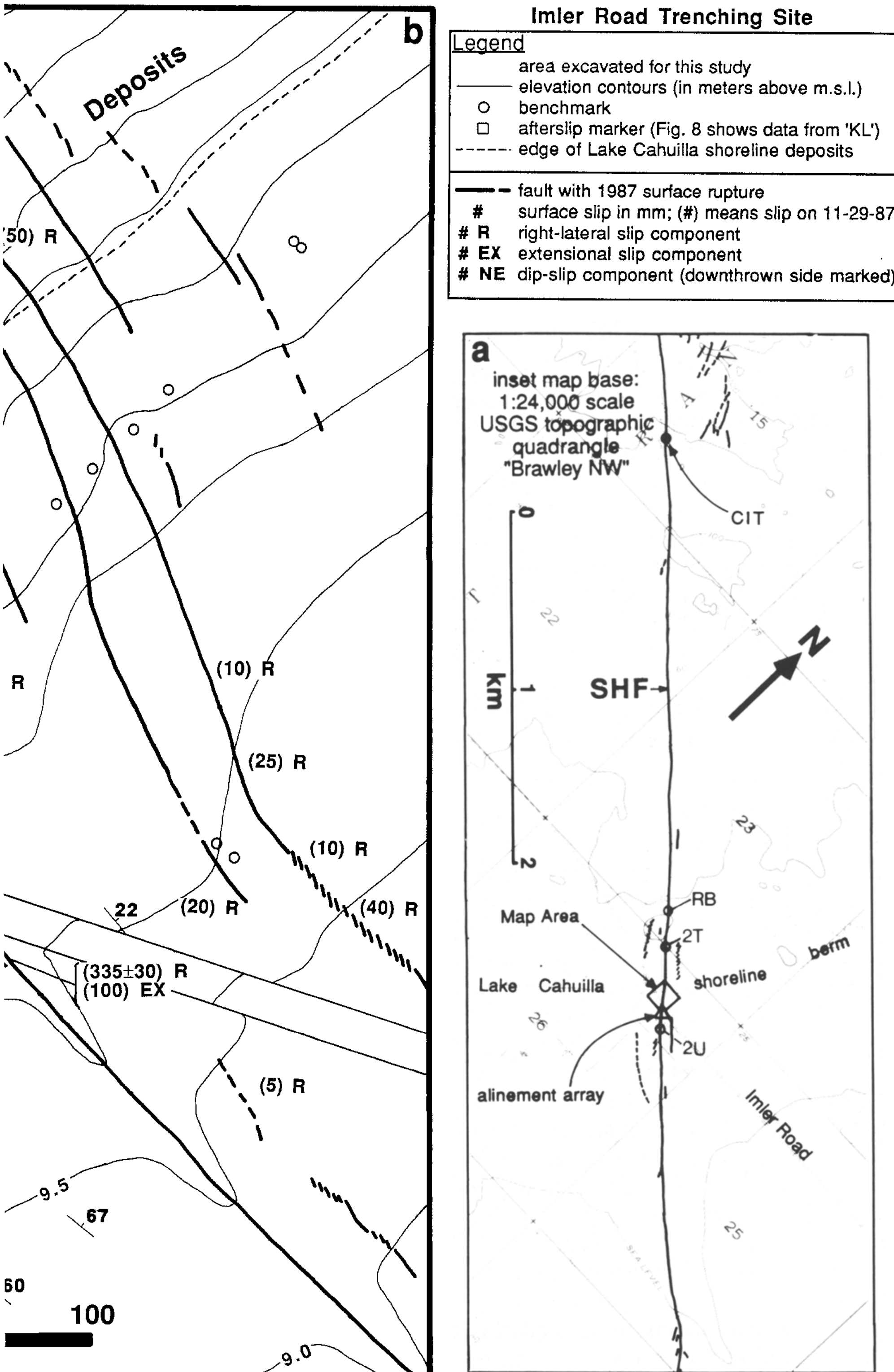
Imler Road Trenching Site
Legend
area excavated for this study
elevation contours (in meters above m.s.l.)
benchmark
afterslip marker (Fig. 8 shows data from 'KL')
edge of Lake Cahuilla shoreline deposits
fault with 1987 surface rupture
surface slip in mm; (#) means slip on 11-29-87
R right-lateral slip component
EX extensional slip component
NE dip-slip component (downthrown side marked)
b
Deposits
(50) R
R
(10) R
(25) R
(10) R
22
(20) R
(40) R
(335±30) R
(100) EX
(5) R
9.5
67
60
100
9.0
a
inset map base:
1:24,000 scale
USGS topographic
quadrangle
"Brawley NW"
CIT
0
1
2
km
SHF
N
RB
Map Area
2T
Lake Cahuilla
shoreline
berm
2U
alinement array
Imler Road

The main body of this paper consists of documentation of our excavations and relevant co-seismic and afterslip data. These data allow us to discuss earthquake recurrence for the fault in terms of recurrence models, and to estimate a long-term slip rate. These data also encourage us to speculate about the significance of historical clustering and northward migration of moderate earthquakes in the region during the past several decades.

Site Description and Documentation

Local Geology

About 5 km northwest of its apparent southern terminus (as mapped before 1987), the Superstition Hills fault crosses the shoreline deposits of Lake Cahuilla that represent its late Holocene high stands (Fig. 1). Figure 2 shows this crossing, about 250 m northwest of Imler Road and just northwest of a dirt road constructed by the U.S. Navy. In this region, the fault plane is bounded on both sides by the late Pleistocene (?) Brawley formation (Dibblee, 1984). Southeast of the Navy road, on the now-desiccated floor of the ancient lake, the fault is expressed geomorphically as a meter-high spine of nearly vertical dipping sandstone. Northwest of the shoreline deposits, and above the level of the ancient lake, the fault appears as a 1.5-m-wide zone of red-brown highly sheared clay bounded by steeply dipping Brawley siltstones and claystones. Before the 1987 earthquake, the trace of the fault was not geomorphically apparent where it crossed the nearly 75-m-wide berm of sandy shoreline deposits of Lake Cahuilla. Field observation of the berm before the earthquake had led us to conclude that dextral offset of this nearly linear berm could not have been more than about 2 m.

Stratigraphy and Sedimentation

On the basis of the stratigraphy of the late Holocene strandline elsewhere around the Imperial and Coachella valleys, we suspected that the strandline deposits at the site would contain many linear geological features that crossed the fault at high angles. At other localities, these features include notches cut into bedrock by waves, the lower boundaries of downlapping beds, the upper boundaries of toplapping beds (Mitchum *et al.*, 1977), and pinchouts of silty lagoonal beds and cobble or pebble lines within the beach deposits. In order to identify specific reference lines at the site that might pierce the fault at high angles, our first excavations were made parallel to, and 2 to 3 m on either side of, the main trace of the fault (Fig. 2).

We also suspected that the strandline deposits would represent the highstand of several late Holocene lakes, not just the most recent one (Sieh, 1986; McGill and Sieh, manuscript in preparation). For this reason, we chose to excavate on the lakeward side of the berm, where the deposits of the youngest lake were most likely to be present. We also chose to excavate only sediments below an elevation of 13 m, because the surface of the latest lake during its highstand was at an elevation of about 12.6 m in this area (Sieh, 1987; F. Webb and K. Sieh, unpublished data).

The fault-parallel trenches revealed several potentially useful reference lines (Fig. 3). We recognized two types of beds: a poorly sorted, slightly indurated, irregularly bedded, surficial carapace of aeolian and bioturbated sand and silt that we here term "colluvium," and a series of lakeward-dipping beach sands that rest upon an abrasion platform cut into the Brawley formation by waves of the most recent lake. Details of the sedimentary features of these deposits are shown in Figure 3.

Seven sets of comformable beds, separated by surfaces that are locally erosional, comprise the beach deposits at this site (Fig. 4). Similar bed geometry and facies

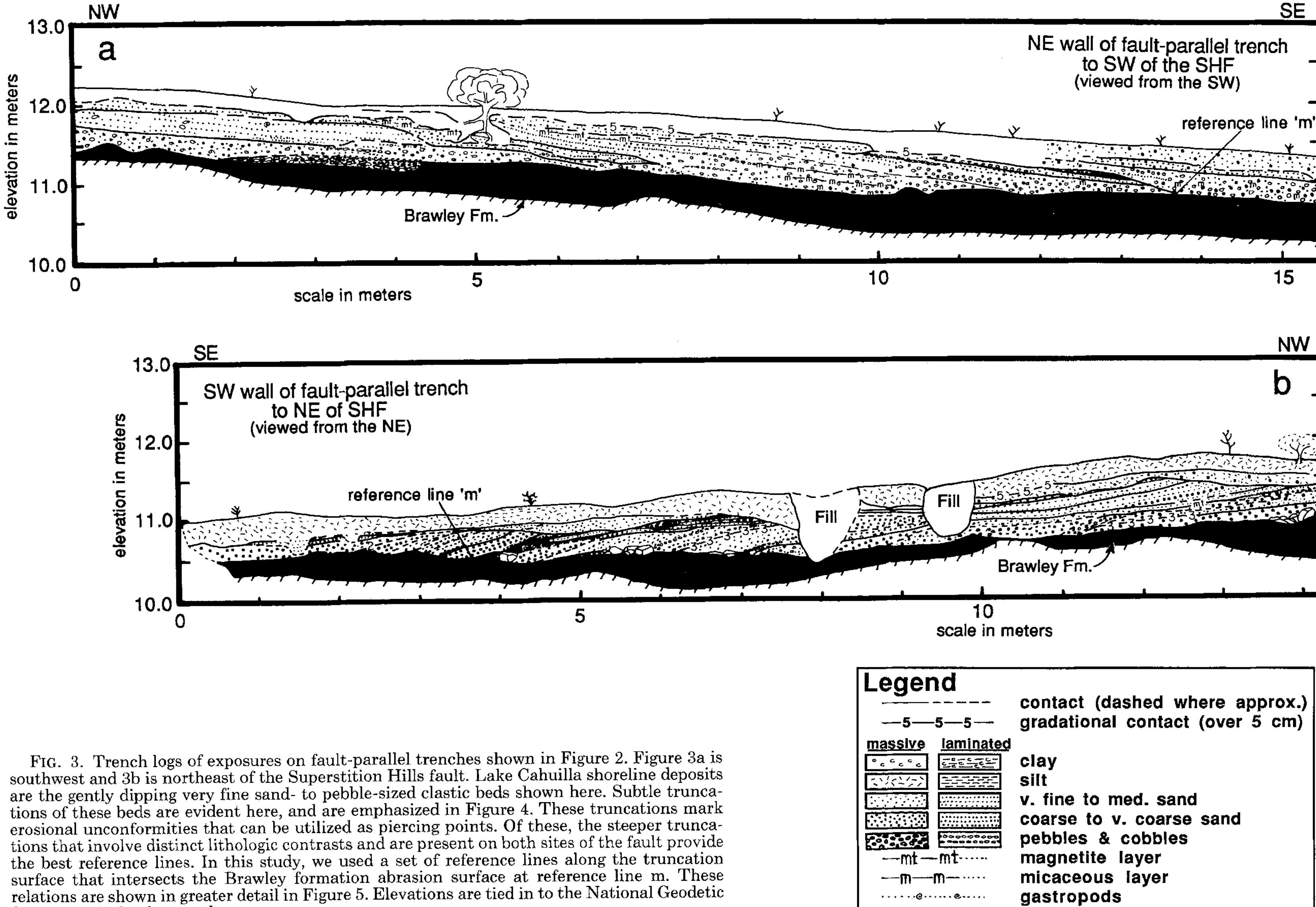

FIG. 3. Trench logs of exposures on fault-parallel trenches shown in Figure 2. Figure 3a is southwest and 3b is northeast of the Superstition Hills fault. Lake Cahuilla shoreline deposits are the gently dipping very fine sand- to pebble-sized clastic beds shown here. Subtle truncations of these beds are evident here, and are emphasized in Figure 4. These truncations mark erosional unconformities that can be utilized as piercing points. Of these, the steeper truncations that involve distinct lithologic contrasts and are present on both sites of the fault provide the best reference lines. In this study, we used a set of reference lines along the truncation surface that intersects the Brawley formation abrasion surface at reference line m. These relations are shown in greater detail in Figure 5. Elevations are tied in to the National Geodetic Survey vertical reference datum.

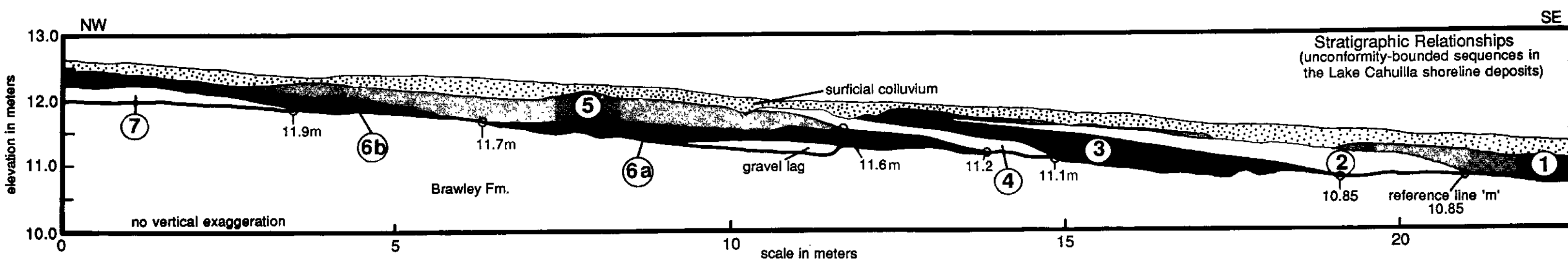

FIG. 4. Stylized view of the Lake Cahuilla shoreline deposits shown in Figure 3. The deposits constitute a series of downlapping beds, bounded by surfaces that generally are unconformable near their upper and lower ends, and disconformable between (refer to Figures 3a and b). These are interpreted here as bedsets (stratigraphically distinct sequences) of sediment. The numbers assigned to these bedsets ascend with increasing age. From the relationships seen in this diagram, it is clear that reference line m is within some of the youngest exposed Lake Cahuilla deposits. These foreset beds were presumably deposited as the lake was receding from its highstand level of 12.6 m above mean sea level. Notches and their approximate elevations (in meters) shown here are interpreted as quiet-water level markers.

changes characterize each of these bedsets (Campbell, 1967). The beds in general are well-sorted yet poorly graded, with lateral facies changes and interlamination between approximately fine- to pebble-sized grains. Overall, these bedsets prograde lakeward and downslope.

Locally, the top of each of these bedsets was eroded before deposition of the overlying bedset. Each erosional surface is associated with a subtle notch. The elevation of each notch is labelled, and the bedsets are numbered 1 through 7 on Figure 4. The notch elevations decrease lakeward as follows: 11.9 m, 11.7 m, 11.6 m, 11.2 m, 11.1 m, 10.85 m, and 10.85 m. These elevations are measured from Figure 4, and thus represent approximate levels from a single exposure. These notches were probably cut by wave action before successive deposition of each bedset, thus their elevations may nearly represent the elevation of the surface of the latest lake during periods of quiet water. The set of downlapping beds that overlies each notch was deposited on the beach foreshore, probably in the same year during which the notch was cut. The time-stratigraphic succession of these units is therefore now established; they monotonically become younger downslope and lakeward.

The lakeward decrease in elevation of the notches and the stratigraphically evident lakeward decrease in age of the bedsets would be the expected consequences of a desiccating lake. The rate of lowering of the lake was probably about 1.5 m/yr (Waters, 1983; Sieh and Williams, manuscript in preparation), and the quiet water elevation of the lake at highstand was about 12.6 m in this area (Sieh, 1987; F. Webb and K. Sieh, unpublished data); hence these notches were probably cut and the beach deposits laid down within 2 yr of the beginning of desiccation of the latest lake. Sieh and Williams (manuscript in preparation) show from radiocarbon dates near Indio and from historical constraints that desiccation began before A.D. 1711 but after A.D. 1641.

Offset Reference Lines

Figures 3 and 4 give the impression that about a dozen reference lines could have been mapped across the fault zone. In the cross-sections, of course, the reference lines crop out as points; for example, reference line m in Figures 3 and 4. We found only five reference lines that were traceable between the two fault-parallel trenches. All five of these are associated either with bedset 1 or the contact between bedsets 1 and 2.

The intersection of the contact between bedsets 1 and 2 with the abrasion platform on the Brawley formation proved to be the most continuous and well-defined reference line. We have called it reference line m. Two reference lines within bedset 1 were traceable across the fault as well: these were "mb," the base of a distinctive micaceous bed (Fig. 5), and "mt," the top of that bed (not shown in Fig. 5 because intersections were not on the logged parts of these exposures). Two truncations of beds in bedset 2, that are visible higher on the contact between bedsets 1 and 2 (points a and b in Fig. 5), were also traceable, but not as near to the fault. For instance, in Figure 5b reference line "a" has been destroyed by fissuring along a secondary fault.

The reference lines were excavated and mapped in stages, as described below. As an example of our method, we discuss the excavation of the reference lines exposed in trench logs of Figures 3a and 5a. The point where reference line m intersected the trench wall in Figure 3a was documented for later measurement by pushing a nail down into the Brawley formation there. The same was done for lines mb and mt. The locations of reference lines a and b were established in a similar fashion, except that the nail heads were placed in the top of the Brawley formation directly

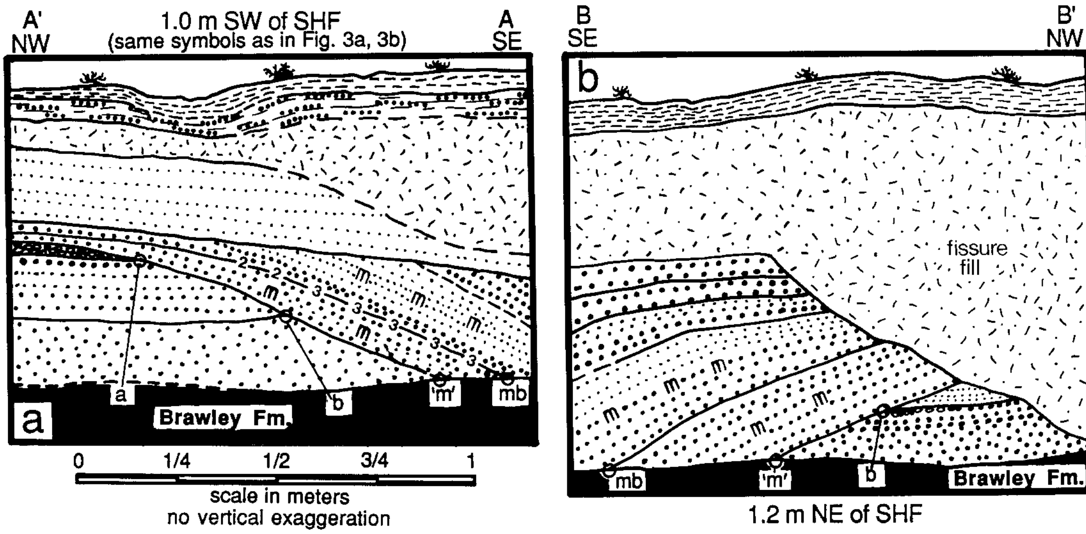

FIG. 5. Detailed logs of exposures between the trenches of Figure 3 and the Superstition Hills fault. The truncation surface between bedset 1 and bedset 2 and the intersection of this surface with the Brawley formation surface at m is clear. Reference lines a, b, mb, and m (see text) intersect these exposures as points.

below the points, because the nails would not have remained in place if they had been left in the sandy contact. The elevations of reference lines a and b were, therefore, not preserved for measurement.

We then proceeded to remove a few centimeters of sand from the wall of the excavation in order to expose the reference lines closer to the fault. Having done so, we sank nails into the Brawley formation at the points where reference lines m and mb intersected it in the new exposure, and into the Brawley formation surface directly beneath the points where the higher reference lines intersected the new exposure. This procedure of excavation down to the surface of the Brawley formation, exposure and then documentation (Fig. 5) of reference lines was done repeatedly, until the reference lines had been excavated completely between the fault-parallel exposures and the main fault. To record the track of each reference line on the unexcavated surface of the Brawley formation, a string was used to connect all exposed points belonging to a single reference line. In the course of this process of three-dimensional excavation, minor sand-filled fissures and scarps of minor faults on the wave-cut surface of the Brawley formation were also discovered and investigated.

Figure 6 is a map displaying the final configuration of the floor of the excavation that exposed the five reference lines. Following complete exposure, all points shown on the map were located using a Zeiss Elta-4 surveying instrument that measures vertical and horizontal angles with an electronic theodolite and slope distance electro-optically. Precision of the measurements with this instrument is about $\leqq \pm$ 3 mm at these short ranges. The same instrument was used for the plane-table mapping shown in Figure 2b.

Figure 6 shows the traces of major and minor faults and fissures on the surface of the Brawley formation, as well as traces of the five reference lines. The faults that break the surface of the Brawley formation and excavated sands are indicated by letters q through z. Letter x signifies the main trace of the Superstition Hills fault.

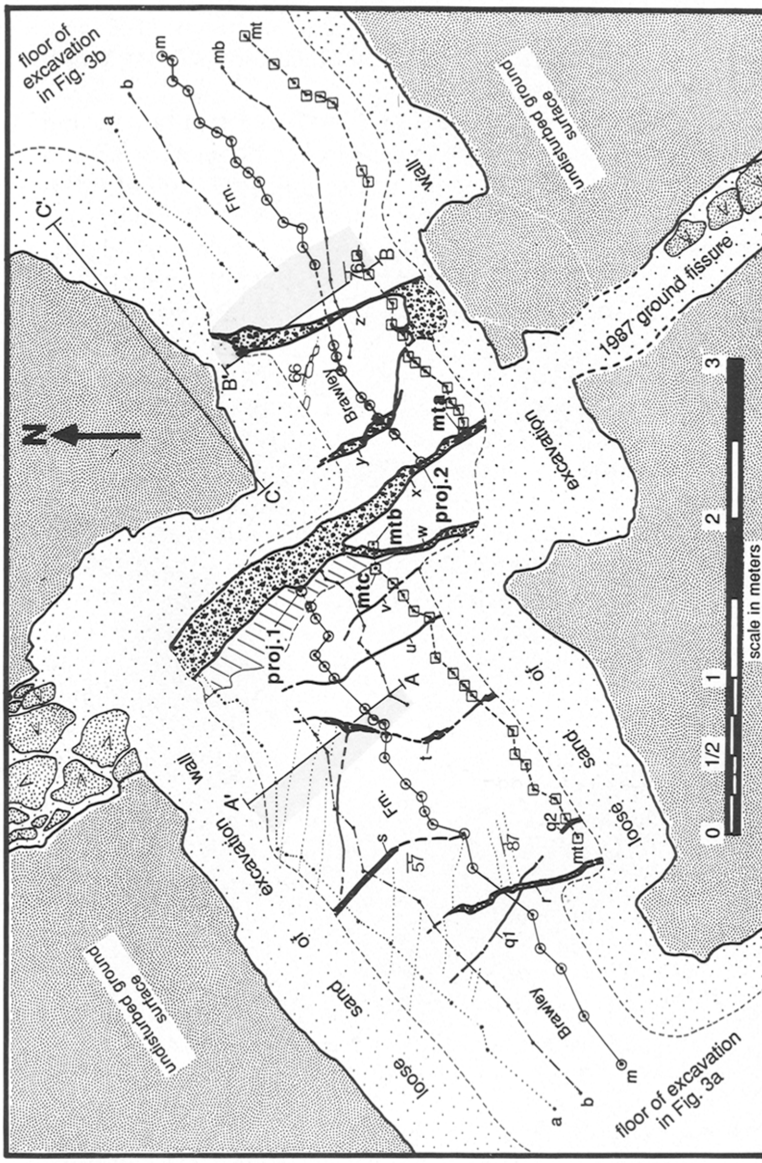

FIG. 6. Map of the traces of reference lines a, b, mb, mt, and m on the exposed surface of the Brawley formation. These reference lines, all of which postdate the latest highstand of Lake Cahuilla, approach the Superstition Hills fault at nearly a right angle. The entire set of reference lines is offset more than a meter across the fault. Faults breaking the Brawley formation are labelled q through z. Fault x is the main strand of the Superstition Hills fault. Hatchured patch southwest of the main strand represents more consolidated fill, probably from earlier fissuring along the fault. Sections A-A′ and B-B′ refer to locations of cross sections shown in Figure 5a and b, respectively. The shaded polygons adjacent to cross-sections A-A′ and B-B′ indicate the map projection of these nonvertical exposures.

Reference line m proved to be the most continuous of the five lines. Even so, m was not present within about 250 mm of the fault, because of erosion relating to fissuring along the main fault plane before 1987. Related fissuring removed lines a and b to distances even farther from the fault. Despite the erosion adjacent to the main fault plane, extrapolation of reference line m to each wall of the fissure along the main fault plane is relatively straightforward.

The vector from point "proj 1" to "proj 2" in Figure 6 is 1115 mm long, and its azimuth is N48.5 ± 0.5°W. The vertical component of this vector is a mere 2.5 mm (northeast side up). Because the fissure walls are uneven this vector does not necessarily represent the true azimuth of the main fault slip vector. The azimuth of the true slip vector is estimated to be N41 ± 7°W, accounting for these irregularities in the fissure walls. Correcting the length of the measured vector for this effect yields a true slip vector shorter by <1 per cent, or about 1106 mm. Uncertainty in the true slip vector azimuth increases the uncertainty in its length by about ±10 mm; other errors are discussed below.

Reference line mt yields a similar offset of 1079 mm, between points mta and mtc. Azimuth of this vector is N59 ± 1.0°W, and the vertical component is 3.5 mm (northeast side up). Minor strand w, however, complicates interpretation of reference line mt near its offset by the main strand of the Superstition Hills fault, so it is less reliable than the offset of line m. Strand w showed negligible dextral slip, but may have decreased the dextral offset between points mta and mtb nevertheless. Two measurements of slip across strand w averaged 40 mm slope distance along an azimuth of N47°E, with a plunge of 37°NE.

The strand y that trends N44°W, and appears to be a branch of strand z, did not rupture in 1987, but had previously slipped a total of 70 ± 15 mm (horizontal distance) along a vector with azimuth N75°W (at letter y in Fig. 6). Vertical offset was 25 ± 5 mm there (SW down). Reference line m is not significantly offset across this strand. Strand z has a vertical separation of 103 ± 5 mm (at B′ in Fig. 6) and trends N20°W. Dextral slip on z is ≦25 mm; this maximum is provided by the negligible offset of reference line mb. Like strand y, strand z did not slip in 1987.

Thus, the important minor faults we encountered during excavation are z, w, and y, all of which break the Lake Cahuilla deposits and have total offsets of several tens of millimeters. Slip on the other minor breaks, q through v, total less than 50 mm of dextral slip. Only q2, r, s, and t were observed to break the Lake Cahuilla sediments, all with vertical separations ≦10 mm. Of these, only s breaks the uppermost colluvium, but it has no vertical separation there, and this strand did not produce mappable surface rupture in 1987.

The errors involved in the above measurements of reference line m and mt offsets come from several sources. The largest error is in locating the piercing points, involving two problems: location and projection of the reference lines, and location and orientation of the fault plane. The point of intersection of the dipping contact tends to flatten as it nears the abrasion platform and because the contact tends to be gradational over about 10 to 20 mm. We have assigned an error of ±30 mm to this imprecision in pinpointing each point along a reference line. An error of about ±10 mm results from projecting reference line m to the edge of the fissure along the main fault, and then another ±10 mm in further projecting it to the estimated true slip vector azimuth. Another error is an almost negligible surveying inaccuracy of at most about ±5 mm. We estimate that the total uncertainty in length of the true slip vector is therefore about ±50 mm. The absolute azimuth of the directly measured vectors is uncertain by less than ±0.5° relative to true north, as checked by direct observation of Polaris.

To summarize the discussion of the data in Fig. 6, we take 1106 ± 50 mm as the best value for the total dextral slip across the main strand of the Superstition Hills fault since deposition of the reference line m about 330 yr ago (and through 3 March 1988). The true azimuth of the slip vector is about N41 ± 7°W, and its vertical component is negligible.

Offsets Measured After the 1987 Earthquake

In order to compare slip previous to the 1987 earthquake with that associated with the 1987 earthquake, we must know the amount of slip near the excavation site that is associated with the 1987 earthquake. Our measurements show that dextral slip varied appreciably along the segment of the fault that crosses the Lake

Cahuilla beach berm (Fig. 2). Because of slip variation along strike, we needed to estimate the amount of co-seismic and postseismic slip as close to the excavated reference lines as possible.

Following the earthquake, we mapped the principal and branching surficial traces of the fault and the many secondary traces that are shown in Figure 2b. Surface rupture data were first obtained at this site on 27 November. Mapping of all breaks and their displacements onto aerial photos was done on 29 November. Displacements across surface ruptures were obtained by measuring and documenting either the slope distance or the full slip vector between matching features on either side of the fault break. Where slip was along local strike, only the slope distance was measured; where visually distinct vertical and/or horizontal separations existed, in most cases the slip vector was measured. Traces of the fault breaks were field mapped and also directly surveyed during the plane-table mapping.

The main fault strand is nearly straight over the whole length shown in Figure 2b. Minor variations in fault strike exist, however, and these are typically associated with local pushups, pull-aparts, fissures, slumps, and minor faults. The segment of the fault next to our excavations undergoes several changes in strike of a few degrees as it crosses the berm. Collapse or slump features and open fissures are associated with these irregularities. These features were particularly abundant between sites labelled station 3 and KL on Figure 2, and between station 7 and station 1.

Of the three breaks that splay from the main trace to the southwest (between the main trace and Navy Road in Fig. 2b), the two closest to the Navy road were the most pronounced, with both dip-slip and dextral slip components of $\geqq$30 mm. These also were observed in October 1988 to be developing into collapse graben along the main trace. The branch fault farther northwest and a solitary branch to the northeast were minor (dip and strike-slip offsets $\leqq$20 mm). None of these branching breaks overlaps along strike with the area, near station 7, in which we did our three-dimensional excavations.

Secondary faults generally followed fold limbs in the Brawley formation, and individually had as much as 50 mm total dextral slip. They do overlap along strike with our excavations, and slip on these strands is considered below in estimating slip rate across the fault zone. These faults also had minor amounts of dip slip and extensional slip. Faults northeast of the main trace of the Superstition Hills fault slipped the greatest amount. Locally, these faults are distributed over a zone and are arcuate in map view, but towards the southeast they coalesce and become subparallel to the main trace. The northwest end of this coalescence is seen in the lower right quadrant of Figure 2, north of the Navy road. All slip on these strands apparently occurred before mapping on 29 November 1987; no afterslip has yet been observed at sites labelled Sta. 4, Sta. 5, and Sta. 6 on Figure 2b, but some could have gone un-noticed before 10 February 1988.

1987 Slip Vector Determination

Measurement of slip vectors across the main trace of the fault were made at three localities on the berm on 27 November and at five localities on 29 November. These determinations were made by measuring the distance across the fault between matching, ephemeral features, at localities where the main trace rupture was a single fracture. Along the ~10 m segment we later excavated, no matching features were found, so we have used the data from location KL (Fig. 2) to estimate 1987 slip and afterslip at the location of our excavations. On 27 November the initial measurement of total slip at site KL was made, and two stakes were driven into the ground, one on each side of the fault. The length of the line between the stakes was also recorded then, but these data were unfortunately lost.

Dextral offsets measured on and near the berm on 29 November ranged from 250 mm (adjacent to a branching strand) up to 400 mm. At this time total dextral slip of 340 ± 5 mm was measured at site KL (co-seismic plus afterslip), but length of that afterslip baseline was not remeasured then. By the time we realized that we had not adequately established the initial slip at KL because of data loss, the matching feature used in that initial measurement could not be recovered. We thus needed to estimate the afterslip at KL that occurred between 27 and 29 November. Extrapolation of data (using either the best-fitting power law or semi-logarithmic function) from the two nearby afterslip sites (2T and 2U in Fig. 2a) of Williams and Magistrale (1989) gives about 29 ± 10 mm of slip during that interval, so the initial offset across KL is estimated as 311 ± 15 mm on 27 November. Afterslip at KL between 27 November 1987 and 3 March 1988 amounted to 186 ± 5 mm. Together, these sum to 497 ± 20 mm. On 3 March, we measured 1106 ± 50 mm of dextral offset of the ~330-year-old reference line m in our excavations.

By 25 October 1988, an additional 79 mm of dextral slip had occurred on afterslip line KL; so the total slip due to the 1987 event and aftercreep was then 576 ± 20 mm. Offset of reference line m on 25 October would have totalled 1185 ± 50 mm. Thus, dextral slip associated with the 1987 earthquake and the first 11 months of afterslip was already approaching the total slip accumulated during the previous 3 centuries.

Creep Before 1987

Only 609 ± 50 mm of dextral slip occurred across the fault at the site of our excavation throughout the 330 years before November 1987. This small amount of previous offset suggests the possibility that all of this slip occurred as creep. For instance, an average creep rate of only 2 mm/yr could have produced the approximately 609 mm of slip in less than 330 years.

During the past 2 decades, the rate of fault creep has been measured at two sites near our excavation. The average rates at these sites are substantially less than 2 mm/yr. At a site 3.15 km northwest of our site, a creepmeter has recorded an average creep rate of about 0.3 mm/yr during the past 2 decades (Louie *et al.*, 1985). All of this creep occurred between installation of the instrument in May 1968 and October 1979. An alignment array immediately southeast of the excavation site (Fig. 2a) recorded only one episode of creep since its installation in 1967, and before November 1987. This was an 18-mm triggered slip event that occurred soon after the Borrego Mountain earthquake of 1968 (McGill *et al.*, 1989). At this time, surface rupture was mapped as a dashed line through the Lake Cahuilla deposits, indicating that surface cracks were seen but no offsets were measured (Allen *et al.*, 1972). No mappable triggered slip occurred within the array or at our site in association with the earthquakes of 1979 or 1981 (Fuis, 1982; Sharp *et al.*, 1986). This is consistent with the observation that no significant offset of the alignment array occurred in association with either event (Louie *et al.*, 1985; McGill *et al.*, 1989). The magnitude of the 1968 creep event divided by the age of the alignment array yields an average slip rate of 0.9 mm/yr.

Prehistoric slip rates cannot be inferred reliably from the 2 decades of instrumental records, although they are one of our only clues to the creep history of the fault at our excavation. If we assume the rate has averaged 0.9 mm/yr for the past 330 yr, about 300 mm of the 609 mm of pre-1987 slip may have accumulated aseismically. Alternatively, if the 1968 event represents the only creep event at the site during the past 330 years, then only 18 of the 609 mm of offset is ascribable to aseismic creep. Finally, from the instrumental record alone, we are unable to exclude the possibility that the instrumental average rates are less than the creep rate averaged over the past 330 years. For instance, lacking evidence other than that presented so far, we could postulate that an event just before deposition of bedsets 1 and 2 (Fig. 4), and followed by afterslip at an initially high rate, produced the full 609 mm of pre-1987 offset of these units.

Slip Before 1968

Was slip before instrumental records of the 1968 triggered slip event mainly a result of creep or of seismic slip? To resolve this ambiguity, we now discuss the history of strand z (Fig. 6). Near the southern boundary of the excavation shown in Figure 6, this feature is dominated by dip slip, with negligible extensional separation or lateral slip. At the northern edge of the excavation, the feature is a fissure with vertical and extensional separation, filled mainly with sand derived from the beds of the latest lake. Surface rupture did not occur along this minor fault during the 1987 earthquake. About 103 ± 5 mm of vertical separation (Fig. 7) has occurred on

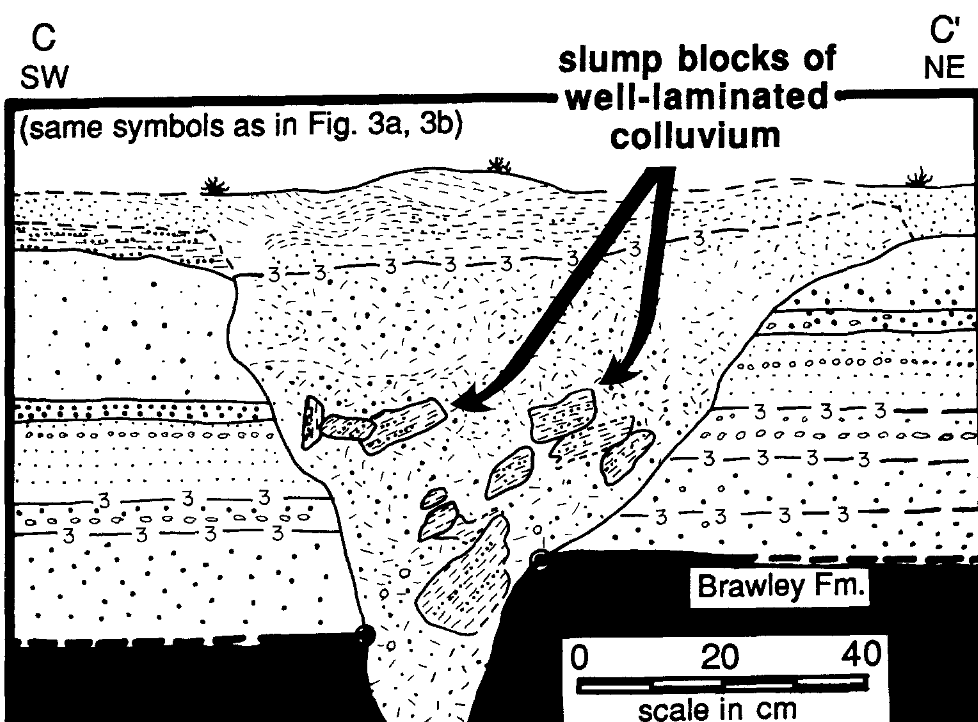

FIG. 7. Exposure of a wedge of colluvium that filled a fissure that overlies the fault strand z that did not rupture in 1987. Vertical separation measured between circled points at the top of the Brawley formation is 103 ± 5 mm. Blocks of the well-laminated colluvium, seen undisturbed in the *upper left* of this section, fell into the fissure, so the fissure formed after deposition of this unit. We interpret this wedge to represent sudden slip on this minor strand. Pre-1987 colluvial wedges similar to this one are also seen along the main SHF, but blocks of colluvium were not found in these exposures. Our interpretation is that these filled collapse pits along the main and minor faults represent a single earthquake that occurred after deposition of the well-laminated colluvium unit.

strand z since deposition of the sands of latest Lake Cahuilla. Reference lines mb and mt display dominantly vertical offset across this structure. No appreciable strike slip occurred on the fault after deposition of these reference lines.

Figure 7 illustrates the cross-section C-C′ that is drawn from the exposure of fault z in the northern wall of the excavation. This outcrop indicates that the loose lake sands collapsed into this fissure over strand z. Section C-C′ through the feature shows an inverted triangular wedge of disturbed lake sands. The sides of the fissure shown in Figure 7 cut the Brawley formation. Sides of the wedge cut the Lake Cahuilla shoreline deposits and an overlying semi-consolidated aeolian and bioturbated sand that we term the "lower, well-laminated unit" of the surficial colluvium. The wedge matrix has no notable fabric, and is composed of mixed sand and silt-sized grains. Blocks within this matrix are the more indurated lower, well-laminated colluvium unit; these blocks are jumbled, yet arranged close to the base of the wedge and generally tilt inwards, towards the center of the wedge.

Figure 7 shows that the fissure formed and was filled after deposition of the lake sands. Also, this fissuring event clearly happened after deposition of about 100 to 200 mm of the lower, well-laminated unit of colluvium atop the lake beds, because intact but friable pebble- and cobble-sized clasts of this unit appear within the poorly sorted sand and silt matrix of the fissure fill. Stratigraphic relations thus establish that the wedge formed not only after deposition of the Lake Cahuilla shoreline deposits, but also after deposition of the lower, well-laminated unit of colluvium.

We have documented this exposure because it may establish whether this wedge developed rapidly or, instead, by incremental opening as would occur with repeated creep events. Clark (1972) documented and interpreted collapse fissures along the Coyote Creek fault trace associated with tectonic slip along that fault, both co-seismic and afterslip. Also, we have observed the fissuring and related effects on main and minor fault strands at the Imler Road site following the 1987 rupture. Based on our observations, we develop some hypothetical considerations and relate these to Clark's work.

First, this type of collapse feature could form suddenly as the fissure opened, creating space into which the loose sands above could fall. The loose Lake Cahuilla sands would presumably cascade from the walls, filling the fissure. The well-laminated unit of colluvium, more indurated than the sands under it, would presumably fragment into blocks, and these blocks would founder or slide down towards the fissure's center. Second, we consider whether the collapse feature could have formed by incremental opening of the fissure. If the fissure opened slightly, some sand would fall in, perhaps producing a slight graben at the surface above. This surficial graben would presumably be filled by a blanket of aeolian deposits. Progressive similar events would probably result in a downdropped graben overlain by laminated aeolian deposits. The lowermost of these deposits would perhaps be faulted by subsequent small slip events. The downdropped center of the graben should show preserved continuity of bedding in the graben, especially in more indurated units. If this hypothetical model of incremental opening represents the process by which the wedge was deposited, then several features we would predict are not observed. Whereas this model predicts that development of the wedge is noncatastrophic, we observe that indurated blocks at the base of the wedge are jumbled, indicating the wedge developed chaotically. We would expect also that the material overlying these blocks would be laminated, as a consequence of incremental deposition of windblown clastic material, but instead we observe the overlying matrix is a massive unit. Also, no faulting of these deposits is observed.

On the basis of these considerations, we favor the model of rapid fissuring and collapse. We proceed by assuming this model is correct. As Clark (1972) showed, collapse fissuring may result from surface water flowing into open ground fractures. He showed that fissures were formed over fractures caused both by creep and by earthquake rupture. Along the Superstition Hills fault following the 1987 event, collapse pits occurred locally. These were caused by opening of tectonic fractures, unassisted by water. Clark observed similar features along the central break of the 1968 rupture. Some fissuring of this type occurred along the main fault trace at our site shortly after the earthquake. For instance, Figure 6 shows blocks of colluvium that fell into a linear collapse feature along the section of the main trace we excavated. Similar fissuring occurred several meters northwest of station KL in Figure 2b.

Collapse fissures similar to ones Clark documented were observed along parts of the 1987 surface break following heavy rains in early February 1988. At our excavation site, however, no collapse fissures of this type had yet developed as of our latest observations in October 1988. We presume that this type of fissuring has not occurred because there is commonly little or no flow of water over the ground surface at this site. Water may instead flow through the porous beach deposits. Perhaps much more severe rains could produce the overland water flow required to produce collapse fissures such as those Clark studied, but this site does not favor such conditions.

As a possible nontectonic cause of the observed collapse feature, we consider piping. This mechanism involves groundwater flow out of fractures at depth, followed by collapse of overlying material. Groundwater withdrawal from open fractures within the fault zone may have accompanied desiccation of Lake Cahuilla. To prove this mechanism, one would have to demonstrate that deposition of the lower, well-laminated colluvium unit occurred within only a few years following the lake's latest highstand.

We consider it probable, although not demonstrated, that pre-1987 minor faulting on strand z and related fissuring occurred in response to movement along the main trace of the fault. Similar branch faults ruptured about 5 and 15 m southeast of the site during the recent earthquake, whereas no such branching has been mapped here associated with the triggered slip events in 1968 and 1979. Also, cross sections through the main fault plane displayed evidence of pre-1987 fissure collapse. Interpretations of exposures of the main fault plane were more ambiguous, however, because of the slope instabilities and sloughing caused by and complexities resulting from movements in 1987.

The incidental evidence given above warrants cautious interpretation, so we have discussed many possibilities. In summary, however, our interpretation of Figure 7 is that the secondary fault strand z probably slipped during a sudden event before 1987, accompanying substantial slip along the main fault at the same time. This earlier slip event produced the collapsed wedge over strand z shown in Figure 7. Although other causes of sudden collapse along this minor strand are possible, we feel this sudden movement represents slip during a moderate earthquake that produced dextral slip of nearly 600 mm on the main trace. Because the fissure above secondary fault z appears to have sustained only one major opening, it may be that most of the pre-1987 dextral slip on the main strand occurred during one slip event.

If more than one major opening had occurred on strand z, we would expect more than one cluster of surficial clasts within the fissure fill. Based on the collapse fissure over this minor strand, and the above reasoning, we discount our previously discussed possibilities for aseismic accumulation of the total pre-1987 offset.

Date of the Pre-1987 Slip

The date (or dates) of the pre-1987 slip is not well constrained. In fact, we know that more than one event is represented by the pre-1987 dextral slip. Eighteen of the approximately 609 mm of pre-1987 slip occurred as triggered slip in 1968. The remaining displacement may have occurred as one, or perhaps more, slip events. We assume in the following discussion that most or all of the pre-1987 dextral slip on the main fault plane occurred during one seismic slip event and subsequent afterslip.

Stratigraphic evidence shows that the event occurred after desiccation had begun, so the pre-1987 event must have occurred after the level of Lake Cahuilla had fallen below an elevation of approximately 10.85 meters, that is, the level of the lake at the time of deposition of the offset reference lines. The lake probably reached this elevation within a year or two of the initiation of desiccation of the lake. From historical records, this desiccation must have begun no later than A.D. 1711 (Sieh and Williams, manuscript in preparation). Two samples of organic debris from plants drowned by the rise of the latest lake near Indio have yielded a radiocarbon date of A.D. 1663 ± 22 (Sieh and Williams, manuscript in preparation). The penultimate slip event clearly occurred during or after this date range.

The historical record of Imperial Valley seismicity precludes the occurrence of major seismic slip along the Superstition Hills fault after mid-1915. However, any of the two moderate earthquakes on 23 June 1915 or the one on 19 April 1906 could conceivably have originated on the fault (Beal, 1915; Townley and Allen, 1939; Toppozada and Parke, 1982). All of these earthquakes were severe in the Imperial Valley, but the scant distribution of felt reports for any of these earthquakes preclude assignment of a specific source. Estimated moments for these two events in 1915 (each was $0.2 * 10^{25}$ dyne*cm; Hanks *et al.*, 1975), however, were apparently much less than the moments of the two largest events in the 1987 sequence (seismic $M_o = 2 * 10^{25}$ and $8 * 10^{25}$ dyne*cm; Bent *et al.*, 1988). Similarly, the 1906 event moment is estimated to have been smaller ($M_o \sim 3 * 10^{25}$ dyne*cm; Hanks *et al.*, 1975) than the 1987 main shock.

A problem with these comparisons is that 1987 moments are derived directly from seismic waveforms, whereas the moment for the 1906 event is based on comparison with the 17 August 1966 event, and the moment for the 1915 events is based on the area over which Modified Mercalli Intensity (MMI) > 6 was felt. To compare the 1906, 1915, and 1987 events, the only directly comparable data for all three is the MMI data that can be compared at specific locations. This comparison is made in Figure 8, in which we have included the 1981 Westmorland earthquake (seismic $M_o \approx 0.1 * 10^{25}$ dyne*cm) for rough calibration.

The 1915 events were felt at the same or greater intensity in most of the Imperial Valley than the 1987 events, while at greater distances the 1915 events were generally less intense. Intensity maps for the 1987 events have yet to be compiled; these maps will allow more accurate comparison of the areas of MMI > 6 for these events. We estimate perhaps a factor of 5 greater area of MMI > 6 for the 1987 events than for the 1915 events, based on comparison of intensities given by

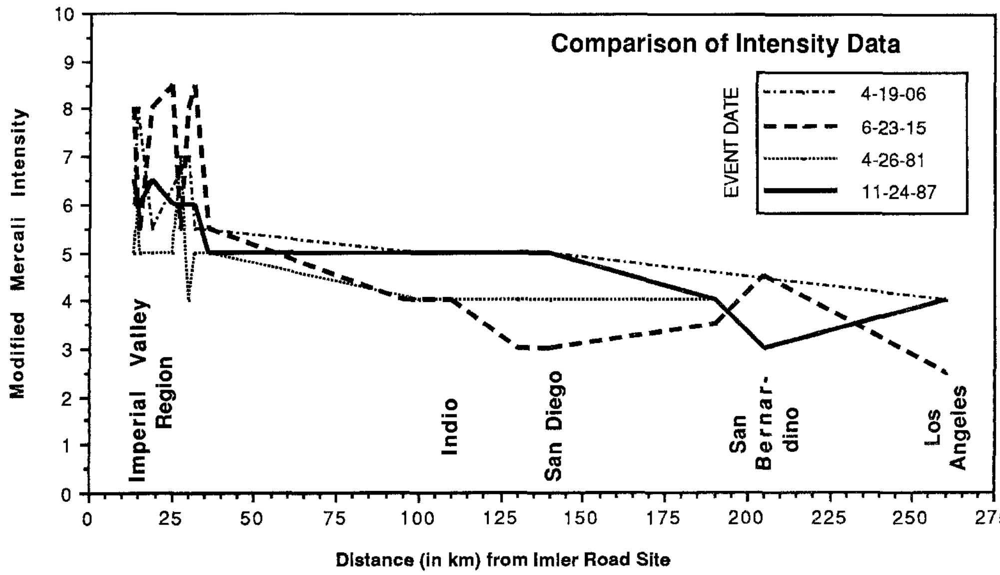

FIG. 8. Direct comparison of the 1906, 1915, 1981, and 1987 events using Modified Mercali Intensity data. Data for the 1906 and 1915 events are from Toppozada and Parke (1982). For the 1981 event, the report in *U.S. Earthquakes* (Stover, 1984) was used. For the 1987 events, Carl Stover (personal comm., 1988) provided prelimary estimates of intensities.

Toppozada and Parke (1982) for the 1915 events and preliminary intensities for the 1987 events (C. Stover, personal comm., 1988). Using our estimate of the largest area of MMI > 6 reasonably allowed by the preliminary intensity data for 1987 of 8000 km^2, the maximum moment for the 1987 event estimated by the method of Hanks *et al.* (1975) is about a factor of 2 less than the seismic moment for the largest event of the 1987 sequence. It therefore seems plausible that the moments for the 1915 events may have also been underestimated by this method. While it appears from comparing intensities that the 1915 events had smaller moments than the 1987 events, our preliminary analysis shows that the 1915 and 1987 sequences were closer in moment than indirect comparison using both seismological and intensity distribution methods would suggest.

The 1906 event produced MMI > 6 over about the same area as the 1915 events (Toppozada and Parke, 1982). In both 1906 and 1981, the highest recorded intensity was near Brawley, with lower intensities reported in El Centro and Imperial. The reports for the 1906 event are very sparse, but at the most distant locations (Yuma, San Diego, and Los Angeles) this event was felt more strongly than the 1915 events, and intensities were the same as for the 1987 events.

In summary, moments for the 1906 and 1915 events are poorly known, and the events are poorly located. Apparently all three events were in the Imperial Valley (Toppozada and Parke, 1982), and the moments of these events may be closer to the moment of the 1987 Superstition Hills main event than indirect comparisons would suggest. It is therefore possible that either the 1906 event or the 1915 event sequence ruptured the Superstition Hills fault. A further possibility is that the first and smaller event of the 1915 sequence ruptured the Elmore Ranch fault, followed by rupture of the Superstition Hills fault, as happened in the 1987 rupture sequence. Of the pair of events in 1915, the Mount Hamilton and Berkeley seismograms showed that the first event was smaller (Townley and Allen, 1939). The separation between the 1915 events was nearly 1 hr.

The date of the pre-1987 slip event is, therefore, now constrained by both maximum and minimum ages. The earliest possible date is A.D. 1641, from radiocarbon dating of the last Lake Cahuilla highstand at Indio. The latest possible date is A.D. 1915, from historical records of earthquakes in the region.

DISCUSSION

Comparison of the 1987 and Pre-1987 Events

On 3 March 1988 when we measured the 1106 ± 50 mm offset of our 330-yr-old reference line, co-seismic and postseismic slip in 1987 and 1988 accounted for 497 mm, or less than half, of the total offset. By 25 October 1988, additional afterslip had increased the total 1987/1988 slip by about 79 mm to nearly half of the total offset since 1660 A.D. By extrapolating our plot of slip at location KL (only ~10 m northwest of our excavations) as a function of time along the best-fitting power-law curve, we estimate that total slip associated with the 1987 event will be about 1210 ± 100 mm by the years 2140 to 2290 A.D., roughly one recurrence interval in the future (Fig. 9). Extrapolation of afterslip has proven to be roughly valid for about a decade following the 1979 Imperial Valley earthquake, and perhaps 2 decades following the 1968 Borrego Mountain event as suggested by Hudnut and Clark (1989). We extrapolate further here with the caveat that simple power law functions may not accurately represent slip accumulation later in the earthquake cycle: the errors stated above attempt to reflect this problem.

This projected value of 1210 mm exceeds the 609 ± 50 mm maximum offset that we determined for the slip event that occurred between about A.D. 1660 and 1915 (plus its afterslip). An extreme hypothesis based upon the data would be that slip in 1987 and subsequent aftercreep nearly equals slip that occurred during the

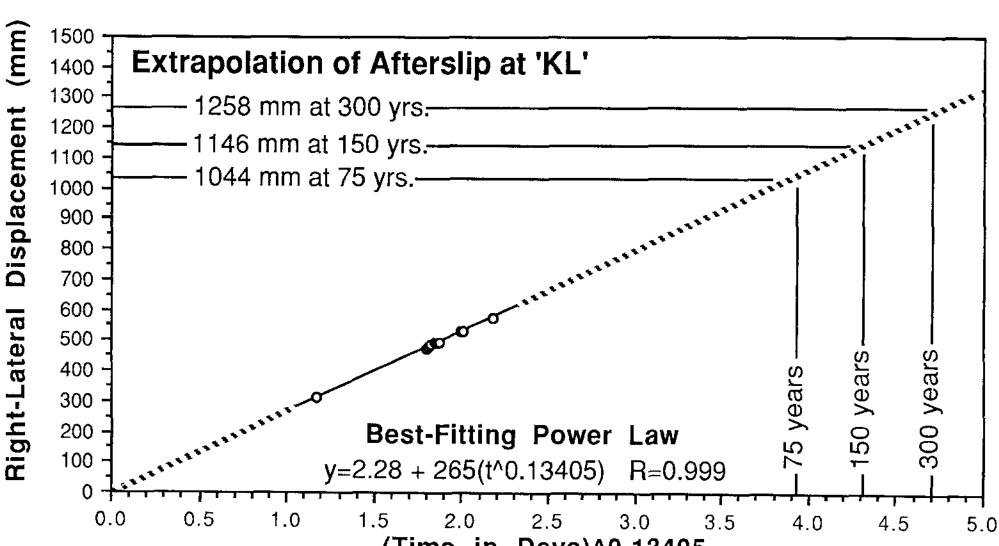

FIG. 9. Extrapolation of afterslip data from the location KL (shown in Fig. 2b) at our trenching site. Projection of our data shows that slip after 150 to 300 yr (the estimated recurrence interval) will total about 1210 ± 100 mm on the main strand of the Superstition Hills fault. Equation for the best-fitting power law function is given (units for calculation are days and millimeters). The time axis is in days after the earthquake, raised to the power of 0.13405. For time reference, the data points (n = 10) are in the period from 27 November 1987 through 25 October 1988. Additional time lines and calculated displacements at each of these times are also shown for reference.

pre-1987 slip event. For the two events to be roughly equivalent, however, almost none of the pre-1968 slip can be atttributable to aseismic creep, and aftercreep rates from the 1987 event must diminish to near-zero by late March 1989 (~480 days after the event).

We predict that the slip associated with the 1987 earthquake and aftercreep will probably eventually be close to the extrapolated 1210 ± 100 mm value, and the amount of slip associated with the penultimate event plus its afterslip is about 609 mm at this site. The 1987 event, therefore, probably involved nearly twice as much slip as the penultimate event, at least at the site of our excavation. The lesser offset at the site during the penultimate event may indicate that the earthquake associated with the pre-1987 slip event was smaller than the 1987 event. If this is the case, it means that this fault does not produce just one size of earthquake. This is an important statement, because the Superstition Hills fault, with its evidently distinct termini, seemed a likely candidate for the generation of characteristic earthquakes. Sharp *et al.* (1989) have, however, mapped previously unrecognized fault breaks farther southeast along strike that occurred along scarps, indicating previous slip. Also, seismological results (Frankel and Wennerberg, 1989) indicate that the rupture process was complex.

To what degree the disparity in slip between events at our single site represents a difference in the sources of the two earthquakes is uncertain. For although offset is known, in general, to increase with rupture length and with earthquake moment magnitude, well-constrained comparisons of slip at the same location during two earthquakes are rare. Perhaps the best study is that of Sharp (1982). He showed that slip along the northern half of the Imperial fault was generally slightly less during the $M_o = 6 * 10^{25}$ dyne*cm earthquake of 1979 than during the $M_o = 56 * 10^{25}$ dyne*cm earthquake of 1940 (Kanamori and Regan, 1982). This partly supports the hypothesis that our site represents less slip and smaller moment for the earlier event on the Superstition Hills fault.

A better, more direct comparison of the size of the 1987 and penultimate events on the Superstition Hills fault may come from offset stream channels (Lindvall *et al.*, 1989). Their data are concentrated between 6 and 16 km from the northwest end of the fault. These data are thus not sufficient to uniquely solve the problem of penultimate rupture length, but they provide constraints on the relative amounts of the 1987 and penultimate event displacements at many other sites. Lindvall *et al.* (1989) show good correspondence between amounts of pre-1987 slip and slip from the November 1987 event through April 1988. This is consistent with our result that November 1987 through May 1988 slip roughly equals total pre-1987 offset of the Lake Cahuilla deposits. If one reasonably assumes that afterslip from the 1987 event will continue over the coming decades, then the characteristic earthquake model (in its strictest sense) does not work for the most recent two events on the Superstition Hills fault.

Recurrence Intervals

Regardless of when in the period between about 1660 and 1915 the penultimate earthquake occurred, the average interval between moderate earthquakes on the Superstition Hills fault is long. If the penultimate event occurred soon after Lake Cahuilla began to dry up, the interval is about 300 yr. If the penultimate slip event at the site represents an earthquake in 1906 or 1915, the average interval is about 150 yr or greater.

Lindvall *et al.* (1989) show evidence for slip events before the penultimate event. Future excavation of older shoreline deposits at our site could test their proposed earlier events, and provide constraints on their dates of occurrence. This future work would also help in refining recurrence interval and slip rate estimates for the Superstition Hills fault.

If the penultimate event occurred as late as 1915, intervals between failures of the Superstition Hills fault must vary markedly. An event in 1915 would have been preceded by an event at least 250 yr earlier, but followed only 72 yr later by another event. This sort of behavior is exhibited by the San Andreas fault at Pallett Creek, where intervals between events vary from about a half century to more than 3 centuries (Sieh *et al.*, 1989).

Slip Rate

The offset 330-yr-old reference line m allows estimation of a slip rate for the Superstition Hills fault. Figures 10a and 10b illustrate probable maximum and minimum rates allowed by our data. In these calculations, the 1987 total slip on the main strand is assigned 576 mm as observed through October 1988, and 1210 mm as predicted from afterslip curves. The penultimate slip event is assigned a total value of 609 mm. In Figure 10a, the penultimate event is assigned its most recent plausible date, 1915. In Figure 10b, its date of occurrence is assumed to be A.D. 1660. The values of slip rate calculated in these two cases are between about 1.7 and 5.5 mm/yr. Calculated values still fall within this range even if: (1) the case in Figure 10a were altered so that the third event back occurs 300 yr earlier, in about A.D. 1360, or (2) the case in Figure 10b were altered so that half of the pre-1987 slip occurs as aseismic slip between 1660 and 1987. Thus, we calculate that the slip rate for just the main trace of the fault as between 1.7 and 5.5 mm/yr at the excavation during the past 330 yr.

This range of values, however, underestimates the slip rate across the entire fault zone. This is because off-fault warping and minor faulting are not taken into account in making the above calculations. The alignment array that straddles the fault just southeast of the excavation encompasses a much wider zone of deformation, also documented by mapping of surficial breaks after the earthquake (Fig. 2). From the mapping and afterslip data presented here, the total slip across the zone may eventually be 1210 ± 100 mm on the main strand plus as much as 110 mm on the minor strands, all of which occurred as discrete surface breaks. McGill *et al.* (1989) discuss data from the adjacent alignment array that showed about 200 mm of slip distributed off of the main strand and across the width of the array within a day after the event. A small amount of additional deformation off the main fault has occurred subsequently as well. Considering all documented afterslip and displacements off of the main strand, displacement across the fault zone at our site from the 1987 earthquake may eventually total about 1410 mm (1210 + 200 mm). That would increase our maximum slip rate estimate to about 6.1 mm/yr. One might further consider additional slip outside the width of the alignment array, and also slip on minor strands and fault branches in the pre-1987 event. These additions would further increase the slip rate for the fault zone. Thus from our data and estimates we obtain a minimum of about 1.7 mm/yr, and a maximum of at least 6.1 mm/yr at this site. Considering the assumptions involved, we state the preferred slip rate estimate as between about 2 and at least 6 mm/yr, with a precision of ±1 mm/yr.

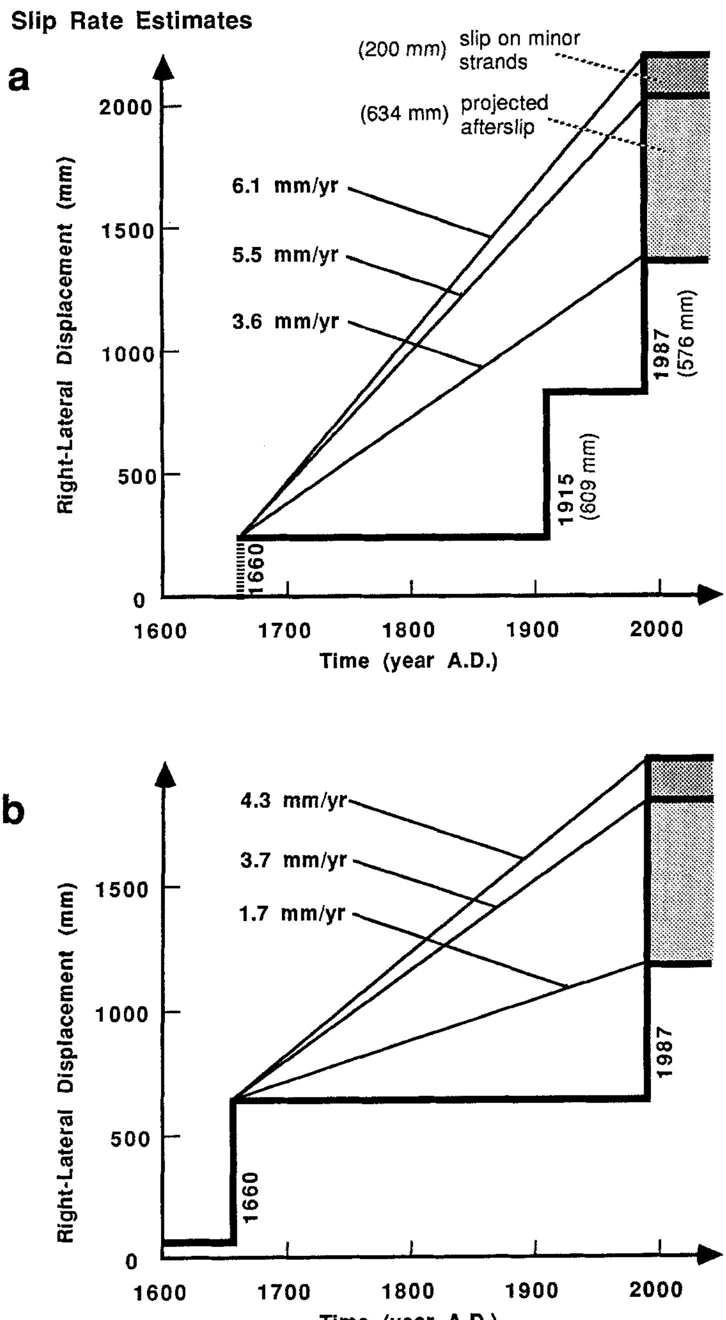

FIG. 10. Illustration of the range of slip rates allowed by data from this study. (a) Penultimate event is assumed to have occurred near the end of the allowable time window, in 1915. The minimum rate is 3.6 mm/yr, based on the assumption that no afterslip will occur after October 1988, and that no displacements occur off the main strand. The maximum rate of 6.1 mm/yr includes both predicted afterslip and observed off-fault slip. (b) Penultimate event is assumed to have occurred about A.D. 1660. Corresponding minima and maxima slip rates are 1.7 mm/yr and 4.3 mm/yr.

For comparison, Sharp (1981) obtained a slip rate of 2.8 to 5.0 mm/yr for a similar time interval on the Coyote Creek fault segment (Fig. 1). In that paper, he also discussed other slip rate estimates for the San Jacinto fault zone. A longer term rate of about 10 ± 2 mm/yr is claimed for the San Jacinto fault zone (Sharp, 1981).

Several reasons may explain why the Superstition Hills fault slip rate is apparently about a factor of 2 lower. First, there is an active strand of the fault zone, the Superstition Mountain fault, that runs subparallel to the Superstition Hills fault, and may itself account for some of the recent slip. This fault is nearly colinear with the Coyote Creek fault, where Sharp (1981) obtained the 2.8 to 5.0 mm/yr slip rate. Second, since we have evidence for only the past 330 yr of slip, it may be that the longer-term rate is not reflected in our estimates. Third, and perhaps most important, the effect of northeast-trending faults in transferring slip between the San Andreas fault and San Jacinto fault zone is not yet well understood. For instance, if these faults bound rotating crustal blocks, the main right-lateral faults on either side of a set of these blocks could have relatively low or variable slip rates.

Implications for Seismic Activity in the Region

All of the known major northwest-trending faults in this region have ruptured during the past several decades, with the exceptions of the Superstition Mountain fault and the San Andreas fault. Also, a northwestward migration of cross-fault ruptures since 1979 has been noticed (Fig. 1 and Hudnut *et al.*, 1989). If indeed the penultimate event on the Superstition Hills fault occurred toward the end of the possible date range between about 1660 and 1915, an important implication may follow. Both it and the Imperial fault (in 1940 and 1979) may thus have ruptured twice in unusually rapid succession. If this represents unusually high activity of these faults, could this and the migration of cross-fault ruptures be phenomena that happen only once every 150 to 300 years? If so, one could further speculate a relation to future rupture of the southern 100 km of the San Andreas fault, which has a similar recurrence interval (Sieh and Williams, manuscript in preparation).

CONCLUSIONS

We present evidence for one seismic slip event on the Superstition Hills fault since about A.D. 1660 and before mid-1915. Also, slip and afterslip in this penultimate event at our site was about half as large as in the 1987 event plus its predicted afterslip. The slip rate at this site has been between about 2 and at least 6 mm/yr for the past 330 yr, and the estimated average recurrence interval is about 150 to 300 yr.

Further, we argue that the characteristic earthquake model probably does not strictly apply to this fault's recent behavior. Monitoring of future afterslip here and at sites studied by Lindvall *et al.* (1989) will presumably resolve this issue. More general models for fault behavior, accounting for significant variability in the earthquake source from one event to the next, seem applicable to the Superstition Hills fault.

ACKNOWLEDGMENTS

L. Gilbert, J. Goodmacher, S. F. McGill, T. Rockwell, L. Seeber, C. Sieh, M. Sigmon, A. Thomas, S. Moore, and D. Valentine all helped with the field effort. We also thank P. Williams and S. F. McGill for afterslip data and data from the Caltech alignment array, respectively. Carl Stover kindly provided preliminary intensity estimates for the 1987 earthquakes. Detailed and helpful reviews were made by M. Clark, N. Christie-Blick, and L. Seeber. Work at this site was done with permission from the U.S. Bureau of Land Management (BLM) and the U.S. Navy. We thank Pat Welch and Lynda Kastoll of the BLM for their assistance. Research was supported by U.S. Geological Survey grants No. 14-08-0001-

G1330 (K.W.H.) and No. 14-08-0001-G1098 (K.E.S.). Lamont-Doherty Geological Observatory contribution No. 4417; Caltech Division of Geological and Planetary Sciences contribution No. 4656.

References

Allen, C. R., M. Wyss, J. Brune, A. Grantz, and R. Wallace (1972). Displacements on the Imperial, Superstition Hills, and San Andreas faults triggered by the Borrego Mountain earthquake, *U.S. Geol. Surv. Profess. Paper 787*, 87–104.

Anderson, J. and P. Bodin (1987). Earthquake recurrence models and historical seismicity in the Mexicali-Imperial Valley, *Bull. Seism. Soc. Am.* **77,** 562–578.

Beal, C. (1915). The earthquake in the Imperial Valley, June 22, 1915, *Bull. Seism. Soc. Am.* **5,** 130–149.

Bent, A., P. Ho-Liu, and D. Helmberger (1988). The November 1987 Superstition Hills earthquake and comparisons with previous neighboring events (abstract), *Seism. Res. Lett.* **59,** 49.

Budding, K. E. and R. V. Sharp (1988). Surface faulting associated with the Elmore Desert Ranch and Superstition Hills, California, earthquakes of 24 November, 1987, *Seism. Res. Lett.* **59,** 49.

Campbell, C. V. (1967). Lamina, laminaset, bed and bedset, *Sedimentology* **8,** 7–26.

Clark, M. M. (1972). Collapse fissures along the Coyote Creek fault, *U.S. Geol. Surv. Profess. Paper 787*, 190–207.

Dibblee, T. W., Jr. (1954). Geology of the Imperial Valley region, California, *Geology of Southern California*, R.H. Johns, Editor, *Calif. Div. Mines. Bull. 170*, p. 21–28.

Dibblee, T. W., Jr. (1984). Stratigraphy and tectonics of the San Felipe Hills, Borrego Badlands, Superstition Hills, and vicinity, in *The Imperial Basin—Tectonics, Sedimentation, and Thermal Aspects: Pacific Section S.E.P.M.*, C. A. Rigsby, Editor, 31–44.

Frankel, A. and L. Wennerberg (1989). Rupture process of the M_s 6.6 Superstition Hills, California, earthquake determined from strong-motion recordings: applications of tomographic source inversion, *Bull. Seism. Soc. Am.* **79**, 515–541.

Fuis, G. (1982). Displacement on the Superstition Hills fault triggered by the earthquake, *U.S. Geol. Surv. Profess. Paper 1254*, 145–154.

Fuis, G. S., W. D. Mooney, J. H. Healey, G. A. McMechan, and W. J. Lutter (1984). Crustal structure of the Imperial Valley region, California, in *The Imperial Basin—Tectonics, Sedimentation, and Thermal Aspects: Pacific Section S.E.P.M.*, C. A. Rigsby, Editor, 1–13.

Hanks, T. C., J. A. Hileman, and W. Thatcher (1975). Seismic moments of the larger earthquakes of the southern California region, *Geol.. Soc. Am. Bull.* **86,** 1131–1139.

Hudnut, K. W. and M. M. Clark (1989). New slip along parts of the 1968 Coyote Creek fault rupture, California, *Bull. Seism. Soc. Am.* **79,** 451–465.

Hudnut, K. W., L. Seeber, and J. Pacheco (1989). Cross-fault triggering in the November 1987 Superstition Hills earthquake sequence, southern California, *Geophys. Res. Letters* **16,** 199–202.

Jacoby, G. C., P. R. Sheppard, and K. E. Sieh (1988). Irregular recurrence of large earthquakes along the San Andreas fault: evidence from trees, *Science* **241,** 196–199.

Johnson, C. E. and L. K. Hutton (1982). Aftershocks and pre-earthquake seismicity, in *The Imperial Valley earthquake of October 15, 1979, U.S. Geol. Surv. Profess. Paper 1254*, 59–76.

Kahle, J. E., C. J. Wills, E. W. Hart, J. A. Treiman, R. B. Greenwood, and R. S. Kaumeyer (1988). Preliminary Report: surface rupture—Superstition Hills earthquakes of November 23 and 24, 1987, *California Geology* **41,** 4, 75–84.

Kanamori, H. and J. Regan (1982). Long-period surface waves, *U.S. Geol. Surv. Profess. Paper 1254*, 55–58.

Lindvall, S., T. Rockwell, and K. Hudnut (1989). Evidence for prehistoric earthquakes on the Superstition Hills fault from offset geomorphic features, *Bull. Seism. Soc. Am.* **79,** 342–361.

Louie, J., C. Allen, D. Johnson, P. Haase, and S. Cohn (1985). Fault slip in southern California, *Bull. Seism. Soc. Am.* **75,** 811–833.

Lomnitz, C., F. Mooser, C. R. Allen, J. N. Brune, and W. Thatcher (1970). Seismicity and tectonics of the northern Gulf of California region, Mexico: preliminary results, *Geofis. Int.* **10,** 37–48.

McGill, S. F., C. R. Allen, K. Hudnut, D. Johnson, W. Miller, and K. E. Sieh (1989). Slip on the Superstition Hills fault and on nearby faults associated with the 24 November 1987 Elmore Desert Ranch and Superstition Hills earthquakes, southern California, *Bull. Seism. Soc. Am.* **79,** 362–375.

McGill, S. F., C. R. Allen, D. Johnson, and K. E. Sieh (1988). Slip on the Superstition Hills fault and on nearby faults associated with the November 23 and 24, 1987, earthquakes southern California, *Seism. Res. Lett.* **59,** 49.

Mitchum, R. M., P. Vail, and S. Thompson (1977). Seismic stratigraphy and global changes of sea level, Part 2: depositional sequences as a basic unit for stratigraphic analysis, in *AAPG Memoir 26,* The American Association of Petroleum Geologists, Tulsa, Oklahoma, 53–62.

Nicholson, C., L. Seeber, P. Williams, and L. Sykes (1986). Seismic evidence for conjugate slip and block rotation within the San Andreas fault system, southern California, *Tectonics* **5,** 629–648.

Sanders, C., H. Magistrale, and H. Kanamori (1986). Rupture patterns and preshocks of large earthquakes in the southern San Jacinto fault zone, *Bull. Seism. Soc. Am.* **76,** 1187–1206.

Schwartz, D. P. and K. J. Coppersmith (1984). Fault behavior and characteristic earthquakes: examples from the Wasatch and San Andreas fault zones, *J. Geophys. Res.* **89,** 5681–5698.

Sharp, R. V. (1981). Variable rates of late Quaternary strike slip on the San Jacinto fault zone, southern California, *J. Geophys. Res.* **86,** 1754–1762.

Sharp, R. V. (1982). Comparison of 1979 surface faulting with earlier displacements in the Imperial Valley, *U.S. Geol. Surv. Profess. Paper 1254,* 213–221.

Sharp, R., M. Rymer, and J. Lienkaemper (1986). Surface displacement on the Imperial and Superstition Hills faults triggered by the Westmorland, California earthquake of 26 April 1981, *Bull. Seism. Soc. Am.* **76,** 949–965.

Sharp, K. E. Budding, G. Boatwright, M. G. Ader, M. G. Bonilla, M. M. Clark, T. E. Fumal, K. K. Harms, J. J. Lienkaemper, D. M. Morton, B. J. O'Neill, C. L. Ostergren, D. J. Ponti, M. J. Rymer, J. L. Saxton, and G. D. Sims (1989). Surface faulting along the Superstition Hills fault zone and nearby faults associated with the earthquakes of 24 November 1987, *Bull. Seism. Soc. Am.* **79,** 252–281.

Sieh, K. E. (1982). Slip along the San Andreas fault associated with the earthquake, *U.S. Geol. Surv. Profess. Paper 1254,* 155–160.

Sieh, K. E. (1986). Slip rate across the San Andreas fault and pre-historic earthquakes at Indio, California, *EOS* **67,** 1200.

Sieh, K. (1987). Earthquake geology of the San Andreas and other faults in California: annual Technical Report, Grant number 14-08-0001-G1098, submitted for publication.

Sieh, K. E., M. Stuiver, and D. Brillinger (1989). A more precise chronology of earthquakes produced by the San Andreas fault in southern California, *J. Geophys. Res.* **94**, 603–623.

Stover, C. (Editor) (1984). *United States Earthquakes, 1981,* U.S.G.S. Special Publication, U.S. Government Printing Office, Washington, D.C., 21–26.

Sykes, L. and Nishenko, S. (1984). Probabilities of occurrence of large plate rupturing earthquakes for the San Andreas, San Jacinto, and Imperial faults, California, 1983–2003, *J. Geophys. Res.* **89,** 5905–5927.

Toppozada, T. and D. Parke (1982). Areas Damaged by California Earthquakes, 1900–1949, *Calif. Div. Mines Geol., Open File Rept. 82-17 SAC,* 65 pp.

Toppozada, T. R., D. Parke, and C. Higgins (1978). Seismicity of California 1900–1931, *CDMG Special report 135.*

Townley, S. D. and M. Allen (1939). Descriptive catalog of earthquakes of the Pacific Coast of the United States, 1769 to 1928, *Bull. Seism. Soc. Am.* **29,** 1–297.

Waters, M. R. (1983). Late Holocene lacrustine chronology and archaeology of ancient Lake Cahuilla, California, *Quaternary Research* **19,** 373–387.

Wesnousky, S. G. (1986). Earthquakes, Quaternary faults, and seismic hazard in California, *J. Geophys. Res.* **91,** 12,587–12,631.

Wesson, R. L. and Nicholson, C. (1988). Intermediate-term, pre-earthquake phenomena in California, 1975–1986 and prelimary forecast of seismicity for the next decade, *Pageoph* **126,** 407–446.

Williams, P. and K. E. Sieh (1987). Decreasing activity of the southernmost San Andreas fault during the past millenium, *GSA Abstracts with Programs,* **19,** 891.

Williams, P. L. and Magistrale, H. W. (1989). Slip along the Superstition Hills fault associated with the 24 November 1987 Superstition Hills, California, earthquake, *Bull. Seism. Soc. Am.* **79,** 390–410.

LAMONT-DOHERTY GEOLOGICAL OBSERVATORY
PALISADES, NEW YORK 10964 AND
DEPARTMENT OF GEOLOGICAL SCIENCES
COLUMBIA UNIVERSITY
NEW YORK, NEW YORK 10027
(K.W.H.)

DIVISION OF GEOLOGICAL AND PLANETARY SCIENCES
CALIFORNIA INSTITUTE OF TECHNOLOGY
PASADENA, CALIFORNIA 91125
(K.E.S.)

Manuscript received 3 October 1988